• Basic Research •

Intraocular pressure control of a novel glaucoma drainage device - *in vitro* and *in vivo* studies

Li-Jun Cui[1], *Di-Chen Li*[2], *Jian Liu*[3], *Lei Zhang*[4], *Yao Xing*[1]

[1]Department of Ophthalmology, the First Affiliated Hospital of Xi'an Jiaotong University, Xi'an 710061, Shaanxi Province, China
[2]Institute of Advanced Manufacturing Technology, School of Mechanical Engineering, Xi'an Jiaotong University, Xi'an 710061, Shaanxi Province, China
[3]Department of Physiology and Pathophysiology, College of Medicine, Xi'an Jiaotong University, Xi'an 710061, Shaanxi Province, China
[4]Department of Cardiovascular Medicine, the Armed Police Corps Hospital of Shaanxi, Xi'an 710054, Shaanxi Province, China
Correspondence to: Li-Jun Cui. Department of Ophthalmology, the First Affiliated Hospital of Xi'an Jiaotong University. No.277, West Yanta Street, Xi'an 710061, Shaanxi Province, China. cuilijun@mail.xjtu.edu.cn
Received: 2017-04-12 Accepted: 2017-06-26

Abstract
● AIM: To evaluate the intraocular pressure (IOP) control of an artificial trabeculum drainage system (ATDS), a newly designed glaucoma drainage device, and postoperative complications in normal rabbit eyes.

● METHODS: Pressure drops in air and fluid of 30 ATDS were measured after being connected to a closed manometric system. Twenty of them were then chosen and implanted randomly into the eyes of 20 rabbits. Postoperative slit-lamp, gonioscopic examination and IOP measurements were recorded periodically. Ultrasound biomicroscopy and B-scan ultrasonography were also used to observe the complications. Eyes were enucleated on day 60.

● RESULTS: Pressure drops of 4.6-9.4 mm Hg were obtained at physiological aqueous flow rates in the tests *in vitro.* The average postoperative IOP of the experimental eyes (11.6-12.8 mm Hg) was lower than the controls significantly (*P*<0.05) at each time point. Complications of hemorrhage (*n*=1), cellulosic exudation (two cases) and local iris congestion (two cases) were observed. The lumina of the devices were devoid of obstructions in all specimens examined and a thin fibrous capsule was found around the endplate.

● CONCLUSION: ATDS reduce IOP effectively. However, further studies on the structure are needed to reduce complications.

● **KEYWORDS:** drainage device; aqueous humor; outflow; intraocular pressure; rabbit
DOI:10.18240/ijo.2017.09.04

Citation: Cui LJ, Li DC, Liu J, Zhang L, Xing Y. Intraocular pressure control of a novel glaucoma drainage device - *in vitro* and *in vivo* studies. *Int J Ophthalmol* 2017;10(9):1354-1360

INTRODUCTION
Glaucoma is the second most common cause of blindness and the leading cause of irreversible blindness[1]. Glaucoma filtration surgery is a fistulizing procedure that provides an alternative drainage route allowing aqueous to escape from the anterior chamber (AC) to the subconjunctiva in order to lower intraocular pressure (IOP), which includes trabeculectomy and drainage implant surgery. Implantation of glaucoma drainage devices (GDDs) has become a standard procedure in various forms of complicated and refractory glaucoma with comparable IOP control and duration of benefit[2-3]. In certain conditions, such as neovascular glaucoma, irido-corneal syndrome, penetrating keratopathy with glaucoma, and glaucoma following retinal detachment surgery, uveitis, or trauma and so on, it is becoming the primary operation[4]. Such devices enable percolation of aqueous liquid through a tube to a filtering plate in the subconjunctival space, to the Schlemm's canal, or to the suprachoroidal space[5].

There have been many contemporary GDDs commercially available[6] since Molteno implant was invented in 1969[7], but success rates of most clinical series were not satisfied[8-9]. There are a number of unsolved clinical drawbacks of existing systems[10]. While partly attributable to the complicated manifestations and strong wound-healing trend of cases typically selected for implantation, various complications also lead to filtration failure[11-14]. The most significant complication related to exposure is endophthalmitis. Others include hypotony, shallow AC, choroidal effusion, suprachoroidal hemorrhage, tube migration and tube obstruction. The origin of most complications can be traced to design inadequacies, poor flow control, lack of set resistance and suboptimal material biocompatibility[3].

In general, there are 2 types of GDDs[3-4,6,15], with or without set resistance mechanism or pressure sensible valve. The valved implants have a pressure-regulating mechanism to minimize overdrainage. The Ahmed glaucoma valve[16-17], in particular, is proved to function as a real valve that closely regulates pressure within a desired range by a variable resistance in response to changes in flow rate. But the potential site for obstruction by inflammatory debris and valve membrane adhesion[18], especially in Asian eyes[19], may cause surgery failure. On the other hand, hypotony caused by the bulk outflow of aqueous in the early postoperative period is much common in valveless implants. The inserted tube dimension is too large to produce resistance when aqueous humor flows through it at physiological rates. The Baerveldt GDD is available with a surface area of 350 mm² and requires temporary flow restriction to avoid early postoperative hypotony[20]. Either a two staged procedure or ligature technique[11,21-23], with or without fenestration of the tube, are therefore required to produce a temporary restriction of flow. However, these methods are sometimes cumbersome and time consuming, and many researchers[23-24] had proved that it was not possible to regulate pressure in a reliable and predictable way merely by constricting the tube lumen.

On the basis of hydrodynamic principles, we developed a new restricted GDD without valve membranes, which is named artificial trabeculum drainage system (ATDS). The main purpose of this study is to evaluate flow characteristics of ATDS, and observe IOP change and complications after implanted in rabbit eyes.

MATERIALS AND METHODS

Artificial Trabeculum Drainage System Following the concept of tube and plate GDD, ATDS consists of a T-shaped silastic tube (Medical Silicon Rubber Technical Institute of Rubber Goods Design Academy, Beijing, China) and a pear-shaped plate (Institute of Advanced Manufacturing Technology, School of Mechanical Engineering, Xi'an Jiaotong University, Xi'an, China) made of medical-grade polyurethane (PUR) (Figure 1).

The T-tube has the same dimension of 600 μm in outer diameter and 300 μm in inner as the single round tube of GDD available in the market. Several micropores, with diameter of 250 μm, distribute to the 6 mm-long horizontal tube to decrease the blockage of the tube (Figure 2).

The pressure confined system (PCS) on the endplate, which is also a silastic tube, with the inner diameter of 80 μm, circles as a certain mode. This mode is selected from several designs in different tube lengths, calibers and circling ways, by calculating and screening step by step using Poiseuille's law, Bernoulli's formula and FLUNT hydrodynamic software. Pressure drop versus flow rate from theoretical calculations is shown as Figure 3. The local pressure impairments caused by 8 angles with different degrees and a diameter change (from 300 μm to 80 μm) are calculated from Bernoulli formula:

$$h_f=\left(\lambda\frac{l}{d}+\sum\zeta\right)\frac{\upsilon^2}{2g}$$

But the summation is too small to disturb the linear correlation because of the slow flow.

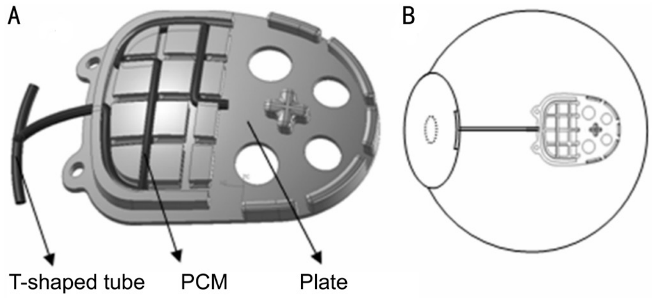

Figure 1 Simulated construction of ATDS A: The medical grade PUR plate, with a spherical undersurface, has an area of 162.2 mm^2. All the evections lying on the posterior plate are designed after analyzing the contact surface between Tenon's capsule and plate using finite element analysis (FEA). Each one has its optimal height, bulk and location to sustain Tenon's capsule and keep the largest drainage surface; B: Location of ATDS.

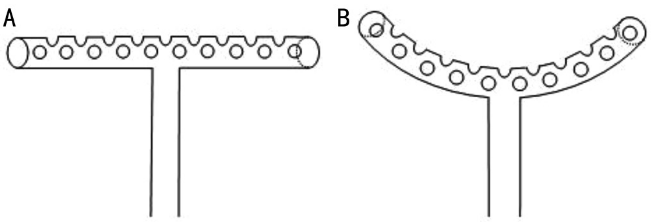

Figure 2 Structure of T-shaped tube The T-shaped tube has an outer diameter of 600 μm and an inner diameter of 300 μm. Many micropores distributing to horizontal tube except the surface connecting with the perpendicular tube (A) are designed to increase the drainage surface and decrease the opportunity of tube obstructed by fibrin clot or iris. When the plate is pulled back, the 5 mm long horizontal tube will curve and match the AC angle (B) to decrease tube movement, prevent extrusion and also block the incision under scleral flap, which consequently, could avoid severe hypotony caused by peritubular filtration.

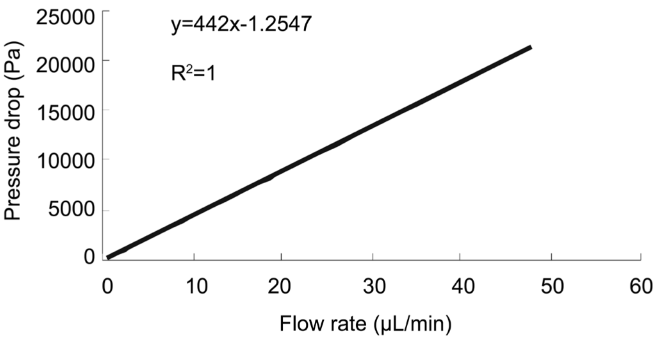

Figure 3 Pressure drops of PCS at different flow rates Pressure drop produced by PCM had a linear correlation with flow rate at a range of 0.6-48.0 μL/min. The pressure drop across straight tube versus flow rate is from Poiseuille's formula[25]: pressure drop=128nlQ/πd^4, where *n*=aqueous viscosity=1.03×10^{-3} NS/m^2; l=length=25.7 mm in this study; Q=aqueous flow rate, d=diameter (metres).

Hydrodynamic Test The characteristic parameters were tested through a flow rig consisted of a tubing compression pump (Model T-Y, TongYi Inc., Shanghai, China), a bridge amplifier (Model ML110, AD Instruments, New South Wales, Australia), a recorder (Model ML200, AD Instruments, New South Wales, Australia), a pressure transducer (Powerlab, AFR Instruments, Tokyo, Japan) and two three-way locks (Figure 4). Pressure changes were recorded and analyzed using Chart 4 software.

Degassed balanced salt solution (BSS) was infused by the pump with initial flow rates preset to 0.6, 1.2, 2.4, 4.8, 9.0, 15.0, 24.0, 48.0 μL/min. All gas bubbles were flushed out when BSS filled all the system. At this point, the two three-way locks were turned to open the system to atmospheric pressure and the pressure reading was zeroed on the recorder. The first three-way lock was then turned to obtain a closed system and the infusion pump was started. The two pressure readings were taken at the same time, and the difference between them was recorded. Repeated flow measurements were taken (n=3). Pressure drops in air and water of 30 ATDSs were tested respectively. Each device was measured during a 10min interval while a constant flow of fluid was pumped into the system.

Experimental Animals A prospective, randomized study was performed using 20 male and female New Zealand White rabbits initially weighing 2.5 to 3.0 kg. The experiment was performed in accordance with the ARVO Statement for the Use of Animals in Ophthalmic and Vision Research. The project was also approved by the Local Animal Research Review committee of the First Affiliated Hospital of Xi'an Jiaotong University, Xi'an, China. All animals were maintained in a 12-hour day and 12-hour night cycle. They were fed and had access to water *ad libitum*.

Twenty ATDSs were implanted into the unilateral eyes of the rabbits. The horizontal part of the T-shaped tube was inserted into the AC while the endplate was placed subconjunctivally posterior to the equator of the eyeball (Figure 1B). The fellow eyes were served as control.

Surgical Procedure After adequate general anesthesia [3% pentobarbital sodium (1.5-2.0 mL/kg) intravenous injection], the eyes were prepared and draped with sterile towels. The lids were secured with a lid speculum. Topical 0.5% tetracaine hydrochloride was instilled to prevent any discomfort. A pair of eye scissors was used to perform a superotemporal limbal peritomy from the 11- to 3-o'clock meridian. A 1-0 silk retention suture was placed around the superior rectus muscle to hold the eyeball and expose the surgical area. Conjunctiva and fascia were separated from the globe and superficial bleeding vessels over the site of the intended scleral flap were cauterized lightly. A rectangle scleral flap measuring 3 mm×5 mm and of one-half scleral thickness was dissected up to the limbal zone from the 1- to 2-o'clock meridian (Figure 5A). A sterile ATDS was put into the subconjunctival space in terms of sliding the plate along the scleral surface. Adequate tube was kept for next step of insertion (Figure 5B). A 2-mm limbal incision was made with a 45° blade. The horizontal tube was folded together by a toothed forceps parallel to the iris plane, and sent into the AC through the limbal incision. It stretched quickly and returned to the original shape under its natural flexibility (Figure 5C). The scleral flap was closed with 4 interrupted 10-0 nylon sutures, 1 each on the sides and apexes. After that, the T-shaped tube was pulled back along the surface of the eyeball to make sure the horizontal tube was close to the anterior chamber angle. Fix the endplate to sclera with 2 interrupted 8-0 nylon sutures through the two semicircle protrusions on the head of the plate (Figure 5D). The

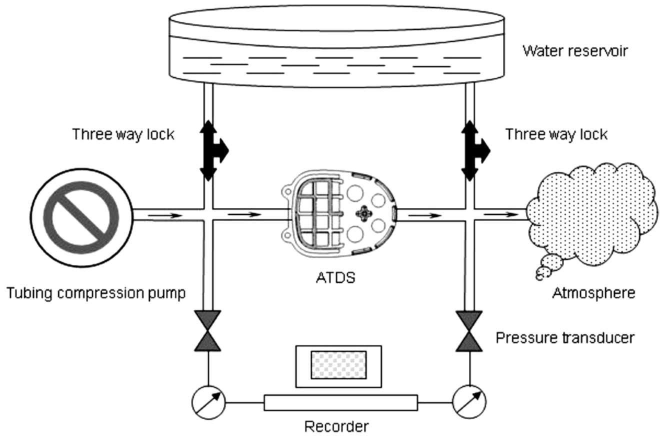

Figure 4 Flow rig for measuring pressure drop Pressure drop were tested in air and water respectively. Repeated flow measurements were taken (n=3), and each device was measured during a 10min interval while a constant flow of fluid was pumped into the system.

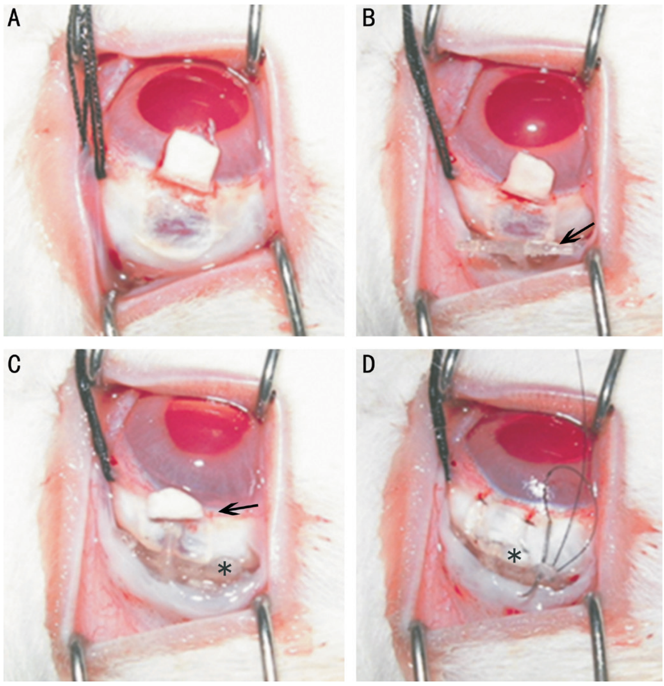

Figure 5 Main procedures of ATDS implanted surgery Arrow shows the T-shaped tube, and asterisk indicates the plate of ATDS.

conjunctival flap was sutured to the limbus with 10-0 nylon suture. Tobradex eyedrop and 0.5% erythromycin ointment were applied into conjunctival sac.

All the surgeries were aseptic and performed by the first author. Tobradex eyedrop was instilled thrice daily for 3d.

Clinical Observation Postoperative evaluations were performed on postoperative days 1-3, 7, 14, 21, 30 and 60, or more frequent when necessary, consisted of general health, Seidal test and red reflex, IOP measurement by Perkins handheld applanation tonometer (HL-2, Kowa, Japan), anterior segments observation by slit-lamp biomicroscopy (SL-8Z, Topcon, Japan) and ultrasound biomicroscopy (UBM, 840, Humphrey, Germany) with a 50 MHz transducer, vitreo-retinal complications by B-scan ultrasonography (SW-2100, Suowei, China) with a 10 MHz probe onto the eyelid after performing methylcellulose. IOP of bilateral eyes at each time point were evaluated using a paired, 2-tailed, Student's *t*-test.

Animals were sacrificed at the end of research (sedation with a lethal dose of intravenous pentobarbital sodium). The ATDS-implanted eyes were enucleated, with care taken not to disturb the tissues around the implant. The appearance of fibrous capsule and the tube lumen were observed.

RESULTS

Hydrodynamic Tests The pressure drops examined at different flow rates correlated closely with that predicted by Poiseuille's formula and Bernoulli's equation (Figure 6). But there was a tendency of larger variation with flow rate increasing.

General State and Intraocular Pressure There was no discharge of all the participants, and red reflex remained normal. There was no significant difference between bilateral baseline IOPs (Table 1), and IOPs of the ATDS-implanted eyes were lower than the controls at each time point (P=0.000). All the eyes were devoid of hypotony. Seidal tests were negative. The variation of bilateral IOPs is shown as Figure 7.

Tissue Responses Illustrated as Figure 8, the thin, lucent and diffused bleb appeared on postoperative days 1 and 3, and it became localized with time. Conjunctival hyperemia triggered by the surgery occurred on day 1 and lightened prominently on day 3 in most of the ATDS-implanted eyes. Cellulosic exudation happened in 2 cases and resolved spontaneously 5 and 7d after implantation. One case of AC hemorrhage occurred on postoperative day 2 (Figure 9). It localized at the tube site, accompanied with moderate corneal edema. The blood was absorbed 1wk after surgery, but corneal edema still existed. Slight iris evection with actiniform vessels injection was found at the tube site in several eyes (11/20). The local iris congestion was slight and resolved in the end, but two of them aggravated at first, and reached its apex as diffuse crimson red on postoperative days 14 and 25. Cornea edema (8/20) was localized at the site of surgery, and 6 of them were

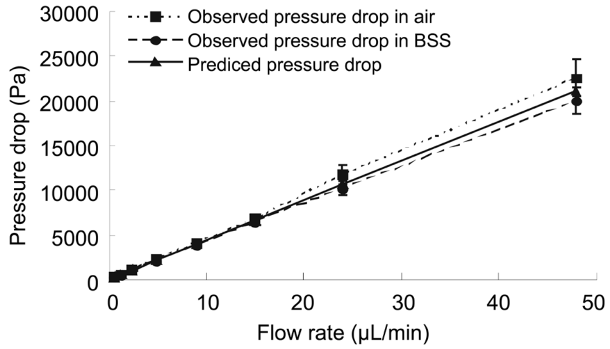

Figure 6 Observed pressure drop versus predicted Fitting linear formula between 0.6 and 48.0 μL/min of the three plots: predicted pressure drop, y=442x-1.2532, R^2=1; observed pressure drop in air, y=473.11x-52.539, R^2=0.9992; observed pressure drop in BSS, y=417.66x+72.411, R^2=0.9998.

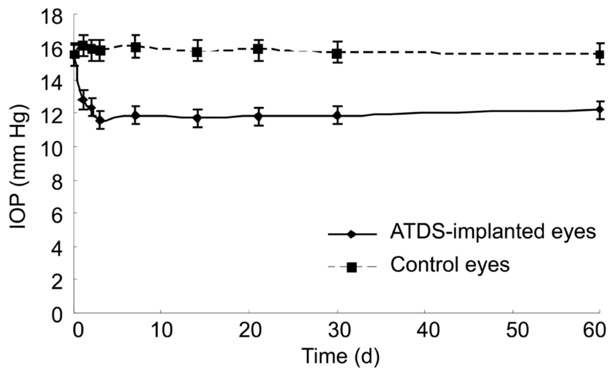

Figure 7 IOP change of bilateral eyes A stable reduction of mean IOP was obtained after it dropped slowly to the average of 11.6 mm Hg 3d after surgery in the ATDS-implanted eyes, and there was no significant difference between consecutive study points.

Table 1 IOPs on each study point

Day	ATDS-implanted eyes	Control eyes	*t*	*P*
0	15.52±0.27	15.55±0.29	-0.860	0.400
1	12.82±0.56	16.08±0.58	-48.913	0.000
2	12.34±0.61	15.85±0.49	-40.909	0.000
3	11.60±0.69	15.81±0.51	-28.664	0.000
7	11.91±0.51	16.02±0.53	-25.482	0.000
14	11.75±0.37	15.73±0.37	-44.853	0.000
21	11.79±0.34	15.84±0.32	-49.635	0.000
30	11.88±0.30	15.67±0.42	-60.134	0.000
60	12.21±0.45	15.60±0.34	-27.270	0.000

accompanied with iris vessel injection. They were resolved 3-15d after implantation. Tube erosion was found in 2 eyes at nearly the end of observations, but the subconjunctival wound healed well and peritubular filtration was not found. No tube migration or extrusion happened in the experimental eyes.

No focal thickening or adherence of cornea and iris was found in the ATDS-implanted eyes in UBM detection. The horizontal part of T-shaped tube was close to the angle of AC (Figure 10A), while the perpendicular part lying straight on the surface of the sclera (Figure 10B). On each time point,

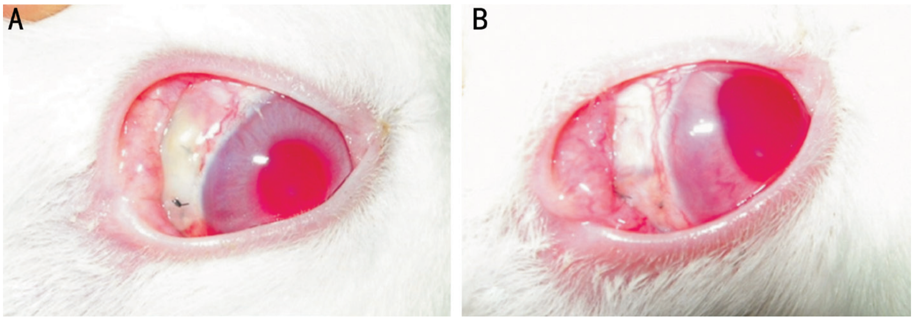

Figure 8 Bleb appearance of ATDS-implanted eyes A: Bleb on postoperative day 3. It was thin, lucent and diffused with slight hyperemia. Only the front part was available; B: Bleb on postoperative day 14. Bleb was thick, transparent ivory white and localized surround the plate.

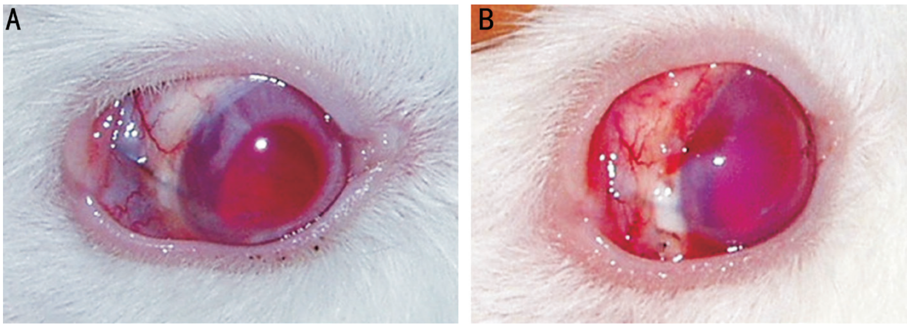

Figure 9 Hemorrhage of anterior chamber A: Slight hemorrhage on postoperative day 2. The T-shaped tube was filled with blood; B: Major part of hemorrhage was absorbed on postoperative day 7, but corneal edema still existed.

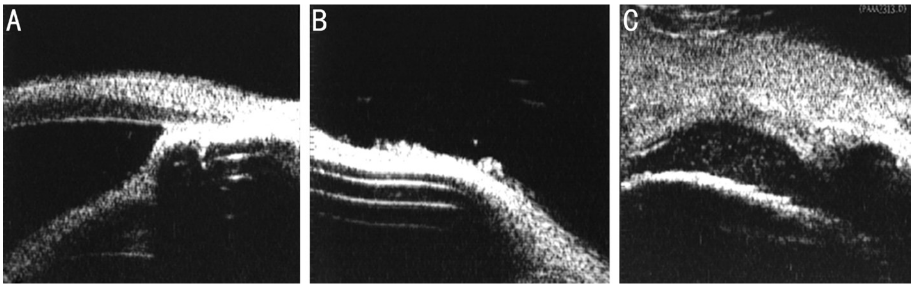

Figure 10 Ultrasound biomicroscopy images The T-shaped tube was hyperechoic in UBM image, with band-shaped sound absorption beneath.

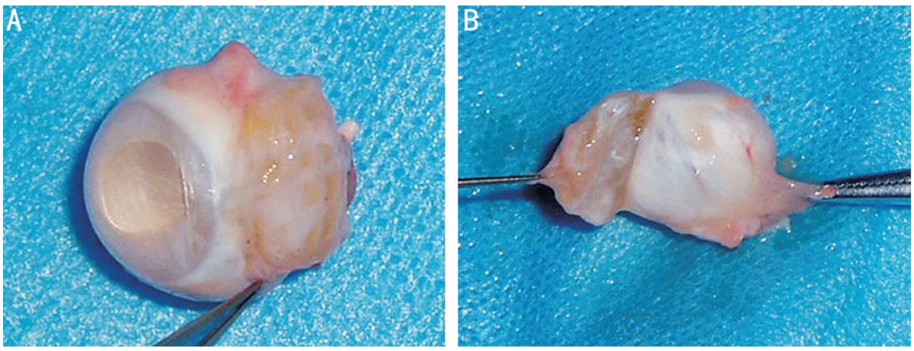

Figure 11 Fibrous capsule in an enucleated eye A: The cornea was transparent, the wound of the limbus healed well; B: The plate was encapsulated by a pink, thin and tenacious fibrous layer including the undersurface connected with the eyeball, and it was easy to separate.

no obstruction was found in tube lumen of all the samples. There was a low echogenic space between bleb tissue and globe, with small punctiform echogenic distribution in the B-scan ultrasonography image (Figure 10C). No ciliary body detachment, suprachoroidal hemorrhage or retinal detachment was found according to the ultrasonography detections.

Enucleated Eyes The local tissue reaction typically consisted of a pink, thin and tenacious capsule. This smooth fibrous layer covered the silastic tube and the endplate of ATDS apparently (Figure 11). A small quantity of fluid flew out when the capsule was opened along the edge of the plate. The lumen of the T-shaped tube and pressure confined mechanism were filled with aqueous humor and devoid of obstructions in all specimens examined, suggesting free flow of fluid.

DISCUSSION

ATDS was developed in accordance with preventing hypotony in routine glaucoma filtration surgery[26], and a new GDD must demonstrate consistent control over internal flowed. The pressure difference between the inlet and outlet of ATDS was mainly influenced by the aqueous flow rate, and produced by frictions of tube wall, resistance of sinuosity, small diameter and sudden dimension change.

According to Energy Conservation Law, conversion of one type of matter into another are always accompanied by the conversion of one form of energy into another. In this study, the potential energy (in form of pressure drop), tube resistance and kinetic energy of aqueous humor are conversed at any time if heat exchange is not under consideration. Consequently, if fluid flows at a steady rate, the pressure of inlet must be higher than that of the outlet to keep the potential energy conversing to the kinetic energy. Pressure drop and flow rate influences each other, and there should be 3 conditions as follows when applying to ATDS: 1) as is shown in the hydrodynamic tests, an 8.5 mm Hg pressure drop will be produced by the pressure confined mechanism when aqueous humor is secreted and drained out at a stable flow rate of 2.5 μL/min, or IOP will be 8.5 mm Hg higher than the inner pressure of the filtration bleb. The success limit of 21 mm Hg needs a steady flow rate of 6.2 μL/min, which is higher than the physiological range of human aqueous secretion; 2) if the pressure difference between AC and filtration bleb is higher than 8.5 mm Hg, the flow rate will grow bigger than aqueous secretion, which will then cause pressure impairment to decrease the pressure drop until the balance of 8.5 mm Hg is back; 3) aqueous humor could flow outside under any pressure lower than 8.5 mm Hg but higher than its hydrostatic pressure. However, the lowest flow rate in normal adult is thought to be 1.4 μL/min during sleep[27], and the resistance of ATDS at that speed is about 5 mm Hg in basis of the experimental flow study. The kinetic energy of aqueous will accumulate gradually with accrescent secretion rate, and conversed to the potential energy continuously. The pressure difference between AC and filtration bleb will elevate in the end.

The good fit between observed pressure drop across specimen ATDS and that predicted by Poiseuille's law and Bernoulli's formula showed a good expected finding, but a tendency of larger variation with increased flow rate was found simultaneously. This may have been attributable to minor accretions of debris within the tube lumens.

In the rabbit experiment, ATDS-implanted eyes showed a significant IOP reduction of 20.9%, 20.5%, 25.3%, 23.3%, 24.3%, 24.0%, 23.5% and 21.3% of the baseline on each time point, respectively. A stable pressure drop was obtained after day 3, when the inflammatory reaction and surgical irritation had already lightened. The reason why IOP fluctuated between 11.3-12.6 mm Hg and was higher than 8.5 mm Hg is that the physiological flow rates of aqueous humor in rabbit is bigger than in human, and the hydrostatic pressure of filtration bleb should be considered.

The complications triggered by the surgery may have been attributable to the larger incision to AC, reject reactions and irritation of the T-shaped tube. The local evection of iris root demonstrated the pressing from the tube. Although the AC angle in rabbit is longer and narrower than in human, the length and the outer diameter of the T-shaped tube should be decreased to reduce the contact and irritation, without hindering the blockage to the cornea incision. It is satisfactory that all the ATDSs were filled with aqueous humor without any obstructions. The micropores distributed to the horizontal tube are thought to be useful to increase drainage surface and avoid tube obstruction. Blockage may happen in some of the micropores, but others are still open to ensure the aqueous humor outflow.

A thin capsule was found around ATDS on day 60. The hygric granular inner surface with aqueous filled, relating to the hypoechoic space in the B-scan ultrasonography and the stable reduction of IOP, suggested a functional filtration bleb. Thin capsules were also found after glaucoma implant inserted in human or rabbit eyes, which consisted of lamellar collagen deposition surrounded by a granulomatous reaction with multinucleate giant cells[28-29].

ATDS has an exclusive surgical procedure and it is not difficult to implant. This study has proved that ATDS could control IOP over internal flowed and provide consistent protection from hypotony in the early postoperative period. With this basal research, we are confident to improve the construction of ATDS and carry out further long-term animal studies including histopathological research in the future.

ACKNOWLEDGEMENTS

Li-Jun Cui conceived and designed the study. Di-Chen Li designed and screened the pressure confined system, and made ATDS to be available. Jian Liu and Lei Zhang contributed to the Hydrodynamic tests. Li-Jun Cui, Lei Zhang and Yao Xing performed the experiments and wrote the paper. All authors read and approved the manuscript. Our team sincerely thanks to Mr. Jun-Tao Ning and Ms. Li-Hua Liu, School of Mechanical Engineering of Xi'an Jiaotong University, for assistance of mode building and manufacture of ATDS.

Foundation: Supported by National Natural Science Foundation of China (No.81300765).

Conflicts of Interest: **Cui LJ,** None; **Li DC,** None; **Liu J,** None; **Zhang L,** None; **Xing Y,** None.

REFERENCES

1 Bourne RR, Taylor HR, Flaxman SR, Keeffe J, Leasher J, Naidoo K, Pesudovs K, White RA, Wong TY, Resnikoff S, Jonas JB; Vision Loss Expert Group of the Global Burden of Disease Study. Number of people blind or visually impaired by glaucoma worldwide and in world regions 1990 - 2010: a meta-analysis. *PLoS One* 2016;11(10):e0162229.

2 Yu DY, Morgan WH, Sun X, Su EN, Cringle SJ, Yu PK, House P, Guo W, Yu X. The critical role of the conjunctiva in glaucoma filtration surgery. *Prog Retin Eye Res* 2009;28(5):303-328.

3 Levinson JD, Giangiacomo AL, Beck AD, Pruett PB, Superak HM, Lynn MJ, Costarides AP. Glaucoma drainage devices: risk of exposure and infection. *Am J Ophthalmol* 2015;160(3):516-521.e2.

4 Chaudhry M, Grover S, Baisakhiya S, Bajaj A, Bhatia MS. Artificial drainage devices for glaucoma surgery: an overview. *Nepal J Ophthalmol* 2012;4(2):295-302.

5 Wischke C, Neffe AT, Hanh BD, Kreiner CF, Sternberg K, Stachs O, Guthoff RF, Lendlein A. A multifunctional bilayered microstent as glaucoma drainage devices. *J Control Release* 2013;172(3):1002-1010.

6 Gedde SJ, Panarelli JF, Banitt MR, Lee RK. Evidenced-based comparison of aqueous shunts. *Curr Opin Ophthalmol* 2013;24(2):87-95.

7 Razeghinejad MR, Spaeth GL. A history of the surgical management of glaucoma. *Optom Vis Sci* 2011;88(1):E39-E47.

8 Molteno AC, Bevin TH, Herbison P, Husni MA. Long-term results of primary trabeculectomies and Molteno implants for primary open-angle glaucoma. *Arch Ophthalmol* 2011;129(11):1444-1450.

9 Hamanaka T, Otora K, Ono K, Ishida N. Long-term results of non-valved glaucoma drainage implant surgery and glaucoma drainage implant combined with trabeculectomy. *Indian J Ophthalmol* 2014;62(9):911-916.

10 Minckler DS, Francis BA, Hodapp EA, Jampel HD, Lin SC, Samples JR, Smith SD, Singh K. Aqueous shunts in glaucoma: a report by the American Academy of Ophthalmology. *Ophthalmology* 2008;115(6):1089-1098.

11 Riva I, Roberti G, Oddone F, Konstas AG, Quaranta L. Ahmed glaucoma valve implant: surgical technique and complications. *Clin Ophthalmol* 2017;11:357-367.

12 Giovingo M. Complications of glaucoma drainage device surgery: a review. *Semin Ophthalmol* 2014;29(5-6):397-402.

13 Lee NY, Hwang HB, Oh SH, Park CK. Efficacy of additional glaucoma drainage device insertion in refractory glaucoma: case series with a systematic literature review and Meta-analysis. *Semin Ophthalmol* 2015;30(5-6):345-351.

14 Bailey AK, Sarkisian SR Jr. Complications of tube implants and their management. *Curr Opin Ophthalmol* 2014;25(2):148-153.

15 Aref AA, Gedde SJ, Budenz DL. Glaucoma drainage implant surgery. *Dev Ophthalmol* 2012;50:37-47.

16 Francis BA, Cortes A, Chen J, Alvarado JA. Characteristics of glaucoma drainage implants during dynamic and steady-state flow conditions. *Ophthalmology* 1998;105(9):1708-1714.

17 Strubbe DT, Gelatt KN, MacKay EO. In vitro flow characteristics of the Ahmed and self-constructed anterior chamber shunts. *Am J Vet Res* 1997;58:1332-1337.

18 Christakis PG, Kalenak JW, Tsai JC, Zurakowski D, Kammer JA, Harasymowycz PJ, Mura JJ, Cantor LB, Ahmed II. The Ahmed versus Baerveldt study: five-year treatment outcomes. *Ophthalmology* 2016;123(10):2093-2102.

19 Wang JC, See JL, Chew PT. Experience with the use of Baerveldt and Ahmed glaucoma drainage implants in an Asian population. *Ophthalmology* 2004;111(7):1383-1388.

20 Momont AC, Stein JD, Lee PP, Weizer JS. Simultaneous placement of 2 glaucoma drainage devices for uncontrolled glaucoma. *Can J Ophthalmol* 2014;49(2):205-209.

21 Kee C. Prevention of early postoperative hypotony by partial ligation of silicone tube in Ahmed glaucoma valve implantation. *J Glaucoma* 2001;10(6):466-469.

22 Tong L, Frazao K，Labree L, Varma R. Intraocular pressure control and complications with two-stage insertion of the Baerveldt implant. *Ophthalmology* 2003;110(2):353-358.

23 Marchini G, Ceruti P, Vizzari G, Toscani M, Amantea C, Tosi R, Marchetti P. Long-term outcomes of a modified technique using the Baerveldt glaucoma implant for the treatment of refractory glaucoma. *J Glaucoma* 2016;25(12):952-958.

24 Kansal S, Moster MR, Kim D, Schmidt CM Jr, Wilson RP, Katz LJ. Effectiveness of nonocclusive ligature and fenestration used in Baerveldt aqueous shunts for early postoperative intraocular pressure control. *J Glaucoma* 2002;11(1):65-70.

25 Saleh JM. *Fluid flow handbook*. New York: McGram-Hill; 2002.

26 Freedman J. What is new after 40y of glaucoma implants. *J Glaucoma* 2010;19(8):504-508.

27 Fitt AD, Gonzalez G. Fluid mechanics of the human eye: aqueous humour flow in the anterior chamber. *Bull Math Biol* 2006;68(1):53-71.

28 Schoenberg ED, Blake DA, Swann FB, Parlin AW, Zurakowski D, Margo CE, Ponnusamy T, John VT, Ayyala RS. Effect of two novel sustained-release drug delivery systems on bleb fibrosis: an in vivo glaucoma drainage device study in a rabbit model. *Transl Vis Sci Technol* 2015;4(3):4.

29 McCluskey P, Molteno A, Wakefield D, Di Girolamo N. Otago Glaucoma Surgery Outcome Study: the pattern of expression of MMPs and TIMPs in bleb capsules surrounding Molteno implants. *Invest Ophthalmol Vis Sci* 2009;50(5):2161-2164.